

1 Sensory target detection at local and global timescales reveals a hierarchy of supramodal  
2 dynamics in the human cortex

3 Maria Niedernhuber<sup>1,2</sup>, Federico Raimondo<sup>3,5,6</sup>, Jacobo D. Sitt<sup>7</sup>, & Tristan A. Bekinschtein<sup>1</sup>

4 <sup>1</sup> Cambridge Consciousness and Cognition Lab, Department of Psychology, University of  
5 Cambridge, Cambridge CB2 3EB, UK

6 <sup>2</sup> Body, Self, and Plasticity Lab, Department of Psychology, University of Zurich, 8050  
7 Zurich, Switzerland

8 <sup>3</sup> Brain and Spine Institute, Pitié Salpêtrière Hospital, 75013 Paris, France

9 <sup>4</sup> National Institute of Health and Medical Research, 75013 Paris, France

10 <sup>5</sup> Institute of Neuroscience and Medicine, Brain & Behaviour (INM-7), Research Centre  
11 Jülich, 52425 Jülich, Germany

12 <sup>6</sup> Institute of Systems Neuroscience, Medical Faculty, Heinrich Heine University Düsseldorf,  
13 40225 Düsseldorf, Germany

14 <sup>7</sup> Sorbonne Université, Institut du Cerveau - Paris Brain Institute - ICM, Inserm, CNRS,  
15 APHP, Hôpital de la Pitié Salpêtrière, 75013 Paris, France

17 Maria Niedernhuber and Federico Raimondo share first authorship. Tristan  
18 Bekinschtein and Jacobo D. Sitt share last authorship.

19 Page number:

20 Abstract word count: 250

21 Introduction word count: 647

22 Discussion word count: 1397

23 Number of figures; 6

24 Preregistration: <https://osf.io/3mqvy/>

25 The authors declare no competing financial interests.

26 The authors made the following contributions. Maria Niedernhuber: Conceptualization,  
27 Data collection, Data analysis, Writing - Original Draft Preparation, Writing - Review &  
28 Editing; Federico Raimondo: Conceptualization, Data collection, Data analysis, Writing -  
29 Review & Editing; Jacobo D. Sitt: Conceptualization, Writing - Review & Editing; Tristan  
30 A. Bekinschtein: Conceptualization, Writing - Review & Editing.

31 Correspondence concerning this article should be addressed to Maria Niedernhuber,  
32 Craik-Marshall Building, 20 Downing Pl, Cambridge CB2 1QW, United Kingdom. E-mail:  
33 mn473@cam.ac.uk

34

## Abstract

35 To ensure survival in a dynamic environment, the human neocortex monitors input streams  
36 forwarded from different sensory organs for important sensory events. Which principles  
37 govern whether different senses share common or modality-specific networks for sensory  
38 target detection? We examined whether complex targets evoke sustained supramodal  
39 activity while simple targets rely on modality-specific networks with short-lived supramodal  
40 contributions. In a series of hierarchical multisensory target detection studies (n=77, of  
41 either sex) using Electroencephalography, we applied a temporal cross-decoding approach to  
42 dissociate supramodal and modality-specific cortical dynamics elicited by rule-based global  
43 and feature-based local sensory deviations within and between the visual, somatosensory and  
44 auditory modality. Our data show that each sense implements a cortical hierarchy which  
45 orchestrates supramodal target detection responses operating on local and global timescales  
46 at successive processing stages. Across different sensory modalities, simple feature-based  
47 sensory deviations presented in temporal vicinity to a monotonous input stream triggered an  
48 MMN-like local negativity which decayed quickly and early whereas complex rule-based  
49 targets tracked across time evoked a P3b-like global ERP response which generalised across  
50 a late time window. Converging results from temporal cross-modality decoding analyses  
51 across different datasets, we reveal that global ERP responses are sustained in a supramodal  
52 higher-order network whereas local ERP responses canonically thought to rely on  
53 modality-specific regions evolve into short-lived supramodal activity. Taken together, our  
54 findings demonstrate that cortical organisation largely follows a gradient in which short-lived  
55 modality-specific as well as supramodal processes dominate local responses whereas  
56 higher-order processes encode temporally extended abstract supramodal information fed  
57 forward from modality-specific cortices.

58 Sensory target detection at local and global timescales reveals a hierarchy of supramodal  
59 dynamics in the human cortex

60

## Significance statement

61        Each sense supports a cortical hierarchy of processes tracking deviant sensory events at  
62    multiple timescales. Conflicting evidence produced a lively debate around which of these  
63    processes are supramodal. Here, we manipulated the temporal complexity of auditory, tactile,  
64    and visual targets to determine whether cortical local and global ERP responses to sensory  
65    targets share cortical dynamics between the senses. Using temporal cross-decoding, we found  
66    that temporally complex targets elicit a supramodal sustained response. Conversely, local  
67    responses to temporally confined targets typically considered modality-specific rely on early  
68    short-lived supramodal activation. Our finding provides evidence for a supramodal gradient  
69    supporting sensory target detection in the cortex, with implications for multiple fields in  
70    which these responses are studied (such as predictive coding, consciousness, and attention).

71

## Introduction

72        The ability to detect deviant sensory events in a stream of predictable stimuli is crucial  
73    for adaptive behaviour. To enable this, each sense relies on a dedicated temporospatial  
74    hierarchy of cortices spanning from primary sensory to associative and frontal areas in which  
75    successive levels encode increasingly abstract sensory information (Çatal, Gomez-Pilar, &  
76    Northoff, 2022; de Lange, Heilbron, & Kok, 2018; Golesorkhi, Gomez-Pilar, Tumati, Fraser,  
77    & Northoff, 2021; Ito, Hearne, & Cole, 2020; Kiebel, Daunizeau, & Friston, 2008; Raut,  
78    Snyder, & Raichle, 2020; Taylor, Hobbs, Burroni, & Siegelmann, 2015; Wengler, Goldberg,  
79    Chahine, & Horga, 2020).

80

      Sensory targets are followed by two cortical responses which can be located on  
81    successive levels of the cortical hierarchy based on their temporal and cognitive properties:  
82    the Mismatch Negativity (MMN) and the P300 (P3a/P3b) complex. The MMN is an early  
83    local negativity associated with temporally proximal sensory change detection in different  
84    sensory modalities

(Allen et al., 2016; Czigler et al., 2006; Mäntysalo & Näätänen, 1987). Canonically considered pre-attentive (Tiitinen, May, Reinikainen, & Näätänen, 1994), the MMN is modulated by attention but resists distraction (Auksztulewicz & Friston, 2015; Chennu et al., 2013). The P3b is a late distributed temporally extended positivity indexing complex targets across sensory modalities (Pegado et al., 2010; Polich, 2007; Yamaguchi & Knight, 1991b, 1991a). Unlike the MMN, the P3b requires attention and memory to track the sensory context surrounding targets (Katayama & Polich, 1998; Polich, 2007; Squires, Petuchowski, Wickens, & Donchin, 1977). Based on these properties, the MMN and P3b can be placed in lower-order and higher-order levels in the cortical hierarchy respectively (Bekinschtein et al., 2009; Chao, Takaura, Wang, Fujii, & Dehaene, 2018; Wacongne et al., 2011).

Earlier work suggests that the prefrontal cortex processes complex, temporally extended targets while the detection of simple, temporally confined targets largely recruits modality-specific areas (Bekinschtein et al., 2009; Cornella, Leung, Grimm, & Escera, 2012; Donner et al., 2000; Ester, Serences, & Awh, 2009; Golesorkhi et al., 2021; Maekawa et al., 2005; Miller, 2009; Wacongne et al., 2011; Wolff et al., 2022). Nevertheless, considerable debate revolves around the extent to which local and global ERP responses to sensory targets rely on supramodal activation patterns. Various studies found the P3b to originate in supramodal, but also modality-specific frontoparietal sources (Dreo, Attia, Pirtóšek, & Repovš, 2017; Halgren et al., 1995; Halgren, Marinkovic, & Chauvel, 1998; Katayama & Polich, 1998; Walz et al., 2013). Primary sensory and inferior frontal sources generate the MMN in different sensory modalities (Akatsuka, Wasaka, Nakata, Kida, & Kakigi, 2007; Garrido, Kilner, Stephan, & Friston, 2009a, 2009b; Näätänen, Simpson, & Loveless, 1982; Ostwald et al., 2012; Pazo-Alvarez, Cadaveira, & Amenedo, 2003; Shen, Smyk, Meltzoff, & Marshall, 2018). Evidence investigating supramodal contributions to the MMN is inconclusive (Chang, Seth, & Roseboom, 2017; Mariola, Baykova, Chang, Seth, & Roseboom, 2019), leaving the question open whether local sensory mismatch responses share common neural signatures between the senses.

112 We hypothesised that global top-down-driven ERP responses to complex targets might  
113 share neural signatures between the senses. In contrast, local bottom-up-driven ERP  
114 responses to simple targets might be supported by early localised modality-specific activity  
115 with only few supramodal contributions. Our approach exploits differences in the  
116 susceptibility of electrophysiological responses to bottom-up and top-down variables to  
117 dissociate their neural dynamics in different levels of the cortical hierarchy. Based on earlier  
118 work elucidating local and global cortical signalling in the auditory hierarchy (Bekinschtein  
119 et al., 2009; Chennu et al., 2016; Phillips et al., 2016; Sitt et al., 2014; Wacongne et al.,  
120 2011). we use multisensory versions of a hierarchical oddball paradigm (“local-global  
121 paradigm”) in which local and global irregularities in the sensory environment elicit P3b-like  
122 global responses as well as MMN-like local responses (Shirazibeheshti et al., 2018). The  
123 local-global paradigm achieves this by manipulating the complexity of the sensory context in  
124 which a stimulus change appears, thereby mapping cortical and perceptual local-global  
125 hierarchies onto each other (Northoff, Wainio-Theberge, & Evers, 2020).

126

## Materials and methods

127 **Participants**

128 We developed two multisensory versions of the local-global paradigm. In the bimodal  
129 version, separate blocks of somatosensory or auditory expectation violations were presented.  
130 In addition to purely visual, somatosensory and auditory blocks, the trimodal version of the  
131 paradigm encompassed blocks in which trials combined inputs from two different sensory  
132 modalities which could either be visual, auditory or somatosensory. Only individuals with no  
133 history of neurological or psychiatric conditions and no tactile and auditory impairment were  
134 recruited into both studies. In addition, individuals with visual impairments were excluded  
135 from participation in the trimodal study. All participants gave written and informed consent.  
136 Data for the bimodal local-global paradigm were collected at the University of Cambridge

137 and obtained ethical approval from the Department of Psychology (CPREC 2014.25). For  
138 the bimodal study, we invited individuals aged 18-35 to participate through the SONA  
139 participant database at the Department of Psychology. We recruited 30 individuals (15/15  
140 female/male, mean+STD age is 24.57(+4.52)) who were paid £10 per hour for a duration  
141 of 3-3.5 hours. The trimodal task was performed at the Centre Nationale de la Recherche  
142 Scientifique (CNRS) in France. Participants for this study were invited through the CNRS  
143 RISC system. Only individuals aged 18-80 were asked to participate in the trimodal study.  
144 Of 54 participants (35 female, mean( $\pm$ STD) age: 25.20( $\pm$ 4.10) years) who participated in  
145 the trimodal study, 7 were excluded due to a recording error. Participants in the trimodal  
146 study were paid €40 for their effort.

147 **Materials**

148 In the trimodal study, auditory stimulation was applied using Etymotic noise-isolating  
149 insert earphones. Eccentric Rotating Mass motors controlled by two Texas Instruments  
150 DRV2605 haptic drivers were employed to deliver vibrotactile stimulation to the wrist. Two  
151 independent 8x8 LED matrices implemented in virtual reality goggles were used to apply  
152 visual inputs isolating visual hemifields. The setup was controlled using an Arduino Zero  
153 board. The bimodal study used auditory inputs generated by mixing three sinusoidal signals  
154 of either 500, 1000, and 2000 Hz (tone type A) or 350, 700, and 1400 Hz (tone type B) in  
155 Matlab R2016 based on (Chennu et al., 2013) and applied using EARTONE 3A insert  
156 earphones. Tactile stimulation was delivered using a custom-made device which applies  
157 mechanical pins to the fingertip with a Saia-Burgess 12.7 mm stroke, 12 v, 4 W DC  
158 push-action solenoid with 0.3-0.6 N force, and no nominal delay after current onset)  
159 controlled by an Arduino Mega board.

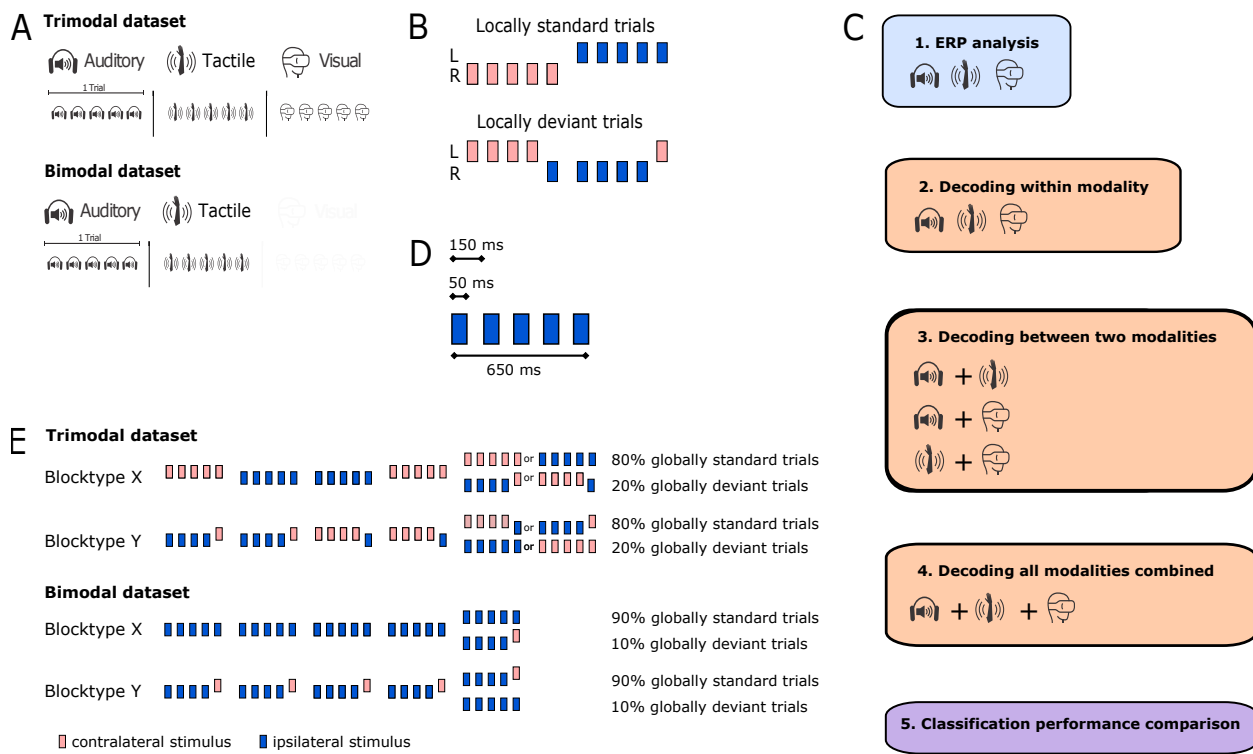


**Figure 1. Experimental design.** Each trial consists of 5 stimuli sampled from one sensory modality. Stimuli could either be auditory, visual or tactile in the trimodal study or auditory and tactile in the bimodal study. For each block, trials sampled from specific sensory modality are presented (A). *Trial design setting up the local contrast between deviant and standard stimuli at trial end:* Standard trials consisted of five identical stimuli applied to the same body hemisphere. Deviant trials were composed of four identical ipsilateral stimuli followed by a contralateral stimulus. In the trimodal study, sensory stimulation started on the left side in 50% of trials for each block. In the bimodal study, trials in 50% of blocks started on the left (B). We first analysed ERP time courses to obtain local and global ERP responses for each contrast. Then, we performed a series of three main temporal decoding analyses for each dataset: First, we decoded the temporal evolution of each local and global ERP response within a sensory modality. We trained and classifiers on one modality to test them on another for each modality pair. In a further step, we trained and tested classifiers on a combination of trial from all sensory modalities for local and global ERP responses separately. Finally, we performed comparisons of classification performance between local and global ERP responses (C). Each stimulus was presented for 50 ms with an inter-stimulus interval of 150 ms. Trials were presented with a jittered inter-trial interval of 1450-1650 ms in the bimodal study and a fixed inter-trial interval of 1400 ms for the trimodal study (D). *Block design setting up the global contrast using nested stimulus groups:* In blocktype X, locally standard trials dominate the input stream and locally deviant trials occur only rarely at a global level. In blocktype Y, this pattern is inverted (E).

160 **Experimental design**

161 We designed two multisensory variants of the local-global oddball paradigm depicted in  
162 Figure 1. In this paradigm, expectations about sensory inputs are violated either locally  
163 within trials or globally between trials. Here, trials were composed of five stimuli with a  
164 stimulus duration of 50 ms and a stimulus onset interval of 150 ms. Each trial consisted of  
165 four identical ipsilateral stimuli followed by a deviant contralateral stimulus (locally deviant  
166 trials) or another ipsilateral stimulus (locally standard trials). Contrasting locally deviant  
167 and standard trials reveals a MMN-like amplitude difference referred to as local ERP  
168 response in a time window between 50-250 ms after onset of the last stimulus in a trial.  
169 Global violations of sensory expectations are achieved when a frequently presented trial type  
170 is occasionally interspersed with a different trial type. A comparison of frequent (globally  
171 standard) trials and rare (globally deviant) trials uncovers a global ERP response which  
172 manifests as a late distributed P3b-like positive wave (Bekinschtein et al., 2009; Chennu et  
173 al., 2013, 2016; Phillips et al., 2016; Sitt et al., 2014; Wacongne et al., 2011).

174 During each study, two block types were presented. The bimodal study consisted of 8  
175 auditory and somatosensory blocks. Standard stimuli in 50% of blocks were presented on the  
176 left side and on the right side in the remaining blocks. Each block consisted of 78% globally  
177 standard trials and 22% globally deviant trials. In block type X, locally standard trials were  
178 occasionally interrupted by 22 % locally deviant trials which could equally likely be a locally  
179 deviant trial in which only the laterality or both laterality and stimulus type were varied. In  
180 block type Y, a stream of locally deviant trials in which the last stimulus was applied to the  
181 contralateral body hemisphere was occasionally interrupted by locally standard trials or  
182 locally deviant trials in which the last stimulus differed in laterality and stimulus type. In  
183 the trimodal study, blocks were composed of 80% globally standard and 20% globally  
184 deviant trials. Trials randomly started on the left or right side within each block with 50%  
185 probability. In blocktype X, locally standard trials consisting of five identical stimuli were

186 interspersed with locally deviant trials in which the last stimulus was applied to the  
187 contralateral hemisphere. Blocktype Y consisted of a sequence of locally deviant trials  
188 occasionally interrupted by locally standard trials. Blocks in both tasks started with a  
189 habituation phase in which the globally standard trial was repeated to establish an  
190 expectation of globally recurring stimulus patterns. We presented 24 repetitions of the  
191 globally standard in the trimodal study and 15 repetitions in the bimodal study.

192 In the bimodal study, somatosensory locally standard trials consisted of five touches  
193 ipsilaterally applied to the index finger. We introduced two types of locally deviant trials in  
194 which the last stimulus in a trial was applied to the contralateral index finger or contralateral  
195 middle finger. In auditory blocks, locally standard trials presented as five identical sounds.  
196 Local deviations were introduced by varying either only the laterality of the ear which  
197 received the last sound in a trial or both the laterality and pitch of the last sound in a trial.  
198 The latter locally deviant trial type was globally deviant type in each block type and the  
199 former locally deviant trial type was globally standard in block type Y and deviant in block  
200 type X. The bimodal study consisted of 8 auditory and 8 somatosensory blocks. The block  
201 order was pseudo-randomised so that the experiment started with somatosensory block type  
202 Y followed by somatosensory block type X, no more than two consecutive blocks were  
203 presented in the same sensory modality, and each half of the experiment contained equal  
204 proportions of somatosensory and auditory blocks. Each block consisted of 158-160 trials  
205 and lasted ~4.5 min. Inter-trial intervals were randomly sampled from a uniform distribution  
206 between 800-1000 ms in steps of 50 ms. In each block, 30-34 globally deviant trials were  
207 embedded in a sequence of 112 globally standard trials and both deviant types occurred in  
208 equal proportions. Each globally deviant trial was preceded either by 2, 3, 4 or 5 globally  
209 standard trials in equal proportions. Participants were exposed to white noise during  
210 somatosensory blocks to avoid auditory cues from the tactile stimulation device.

211 The trimodal study contained blocks with exclusively auditory, visual or somatosensory  
212 stimulation. Participants in this study also underwent multisensory blocks in which

expectations violations require to converge inputs from two of these sensory modalities and which were not further analysed. Local deviations were introduced by varying the laterality of the last stimulus in a trial. 50% of trials applied standard stimuli to the left hemisphere (ear, visual hemifield, or wrist) and the last stimulus to the right hemisphere (and vice versa). Participants underwent three experimental sessions with a total duration of 20 min (4.5 min per session). The remaining two sessions applied crossmodal stimulation and analyses were not included in this paper. 16 participants were presented with somatosensory blocks, 15 participants with auditory blocks and 16 participants with visual blocks. Each block type was presented twice per session in a fixed order: X-Y-X-Y. 31 (~20%) trials included in each block were globally deviant. Each globally deviant trial was preceded by 3, 4, or 5 globally standard trials. To ensure that participants attend to the global regularity in sensory stimulation patterns, we instructed them to count the number of deviant stimulus groups occurring in a stimulus stream and report the number after each block. Blocks in which participants deviated from the true count by more than two were repeated.

## 227 Statistical analysis

EEG data acquisition was performed using a Net Amps 300 amplifier with an Electrical Geodesics 256-channel high density EEG net at the ICM in Paris for the trimodal study and an Electrical Geodesics 128-channel high density EEG net at the Department of Psychology, University of Cambridge for the bimodal study. We performed EEG data preprocessing using EEGLAB 2019 in Matlab 2019b. In a first step, data were down-sampled to 250 Hz, filtered between 0.5-30 Hz and epoched with respect to the onset of the last stimulus in a trial. Habituation trials at the start of each block were removed. Having removed electrodes placed on the neck and cheek which record mostly muscle artefacts, we retained 91 electrodes in the bimodal data set and 175 electrodes in the trimodal data set for further analysis. We performed baseline removal using a window of 100 ms before epoch onset. Noisy trials (with a variance of >350) and channels (with a variance

239 of  $>500$  were temporarily removed using a semi-automated procedure. We removed  
240 artefacts resulting from sweat, eye and muscle movements using independent component  
241 analysis. Ultimately, we removed the remaining artefacts using trial-wise interpolation.

242 We performed cluster-based permutation analyses to test for differences in ERP  
243 amplitude time courses. We used the Common Average as a reference and performed a  
244 baseline correction in a time window of 100 ms before onset of the last stimulus in a trial.  
245 For each condition pair with unequal trial numbers, trials in the condition with a higher trial  
246 number were randomly deselected until the number of trials in both conditions was equal.  
247 Cluster-based permutation uses Monte Carlo partitioning to obtain a cluster-level t-statistic.  
248 To perform Monte Carlo partitioning, data are pooled and randomly divided into two new  
249 data sets of equal size. We performed two-sided t-tests on the subject averages time-channel  
250 pairs and retained only t-values with  $p < 0.05$ . Spatiotemporally adjacent t-values were  
251 summarised and the largest cluster-level summarised t-value was identified. Having  
252 performed this procedure 3000 times, we determined the p-value corresponding to the  
253 proportion of maximal cluster-level t-values larger than the observed t-value in the original  
254 comparison. Conditions were deemed to be different if  $p < 0.05$  (Oostenveld, Fries, Maris, &  
255 Schoffelen, 2011).

256 We applied temporal decoding to examine whether two contrasts rely on similar  
257 cortical signatures. Temporal decoding is a machine learning procedure which assesses  
258 whether a classifier trained to discriminate two trial types at one time point will generalise to  
259 the remaining time points in a sample. We applied a bootstrapping procedure in which 5  
260 trials were randomly sampled from each dataset until we reached 540 epoch averages for each  
261 trial type (deviant/standard) respectively. This procedure was repeated 50 times.  
262 Classification performance was assessed on each of the resulting datasets. To perform  
263 temporal decoding within a sensory modality, we used a 5-fold stratified cross-validation  
264 procedure in which linear support vector machines were trained to optimally separate  
265 standard and deviant trials on 4/5 of the data set and tested on the remaining data. For

266 temporal decoding between sensory modalities, we fitted classifiers using training and testing  
267 datasets from two different sensory modalities. For each condition pair, we trained and  
268 tested classifiers on every time point in a time window of 600 ms after onset of the last  
269 stimulus in a trial. Classification performance was assessed using the Area Under the Curve  
270 Receiver Operating Characteristic (AUC-ROC) which is a non-parametric criterion-free  
271 measure of separability. This procedure results in a training time vs testing time temporal  
272 generalisation matrix with AUC-ROC classification scores as cells. To identify adjacent  
273 AUC-ROC scores which differ from chance, we performed a Monte Carlo cluster-based  
274 permutation analysis with 1024 random partitions on classification score averages from each  
275 bootstrapped dataset and applied two-tailed paired t-tests to identify clusters of AUC-ROC  
276 values ( $p < 0.05$ ) which differ from chance (King & Dehaene, 2014; King, Gramfort,  
277 Schurger, Naccache, & Dehaene, 2014).

278

## Results

279 **Hierarchically nested sensory deviations elicit local and global ERP responses in**  
280 **different sensory modalities**

281 We investigated commonalities in cortical responses to rule-based global and  
282 feature-based local sensory deviations using multisensory versions of the local-global  
283 paradigm.

284 In a first step, we established that hierarchical manipulations of sensory context elicit a  
285 MMN-like local ERP response and a P3b-like global ERP response in the auditory,  
286 somatosensory and visual modality in both experiments. To that end, we performed  
287 cluster-based permutation of ERP amplitude time courses (Maris & Oostenveld, 2007)  
288 displayed in Figure 2. Replicating earlier findings (Bekinschtein et al., 2009; Chennu et al.,  
289 2013), the auditory local ERP response in the bimodal paradigm manifested as a  
290 frontotemporal bipolar two-peak difference wave (cluster  $t = -12000$ ,  $p < 0.001$ ) and a

291 one-peak difference wave in the trimodal paradigm (cluster  $t = -5396.6$ ,  $p < 0.001$ ). A  
292 somatosensory local ERP response emerged as a central negativity between  $\sim 50$ -150 ms in  
293 the bimodal paradigm (cluster  $t = -752.31$ ,  $p < 0.001$ ) and as a two-peak negativity between  
294  $\sim 100$ -350 ms the trimodal paradigm (cluster  $t = -3298.4$ ,  $p < 0.001$ ). We also identified a  
295 visual local ERP response as a negativity in a mid-range time window between  $\sim 100$ -350 ms  
296 (cluster  $t = -6178.9$ ,  $p < 0.001$ ) shown in Figure 2.

297 A comparison of globally deviant and standard trials revealed a positive difference  
298 wave in a time window from  $\sim 250$  ms until the end of the trial regardless of sensory modality  
299 (with some shifts in onset of the effect). In the bimodal (cluster  $t = 22143$ ,  $p < 0.001$ ) and  
300 trimodal study (cluster  $t = 27934$ ,  $p < 0.001$ ), we revealed an auditory global ERP response  
301 as a positive deflection with a posterior distribution. A somatosensory global ERP response  
302 presented with a similar posterior distribution in both the bimodal (cluster  $t = 18351$ ,  $p <$   
303 0.001) and trimodal study (cluster  $t = 21421$ ,  $p < 0.001$ ). Ultimately, a visual global ERP  
304 response emerged as a positive difference wave in a relatively late time window from  $\sim 400$  ms  
305 until the end of the trial (cluster  $t = 12857$ ,  $p < 0.001$ ) shown in Figure 2. These results  
306 show that complex targets which require the conscious tracking of sensory patterns across  
307 time elicit a global ERP response in different sensory modalities. Our finding that the global  
308 ERP response manifests as a large, late and posterior positive deflection regardless of sensory  
309 modality complements previous studies which characterise the related P300 as a late  
310 positivity (Bekinschtein et al., 2009; Bledowski et al., 2004; Chennu et al., 2013; Walz et al.,  
311 2013). Taken together, our results show that the functional dissociation of local and global  
312 ERP responses is a supramodal property of target detection systems in different sensory  
313 domains.

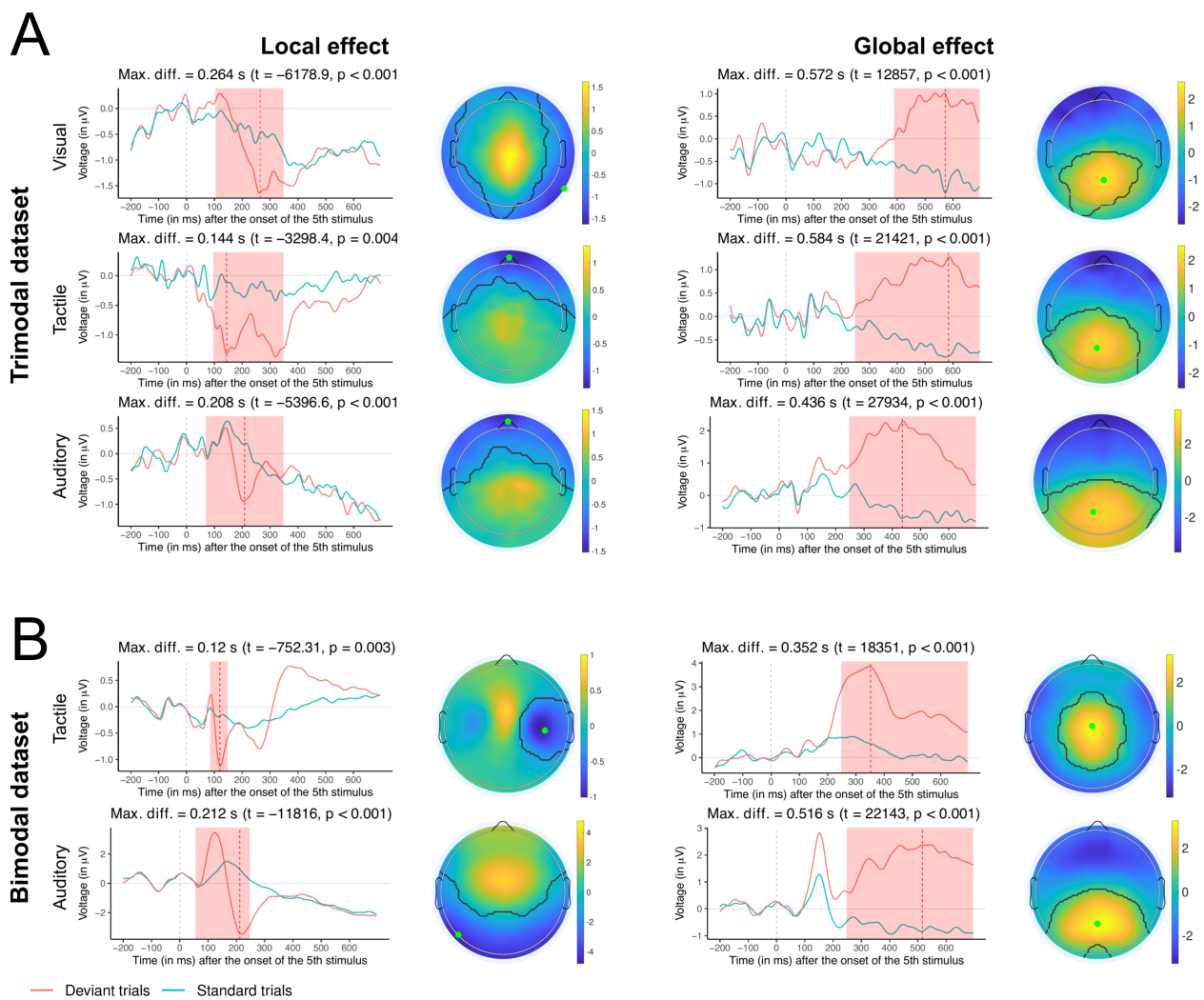


**Figure 2. Experimental design and ERP results.** Cluster-based permutation test results for ERP amplitude differences showing that a local and global ERP response can be obtained in different sensory modalities for the trimodal (A) and the bimodal study (B). On the left, each panel shows ERP amplitude time courses of the corresponding deviant-standard condition pair. Next to the ERP voltage time course plot, the corresponding topographical map is shown. Time periods in which a cluster-based permutation test identified a difference between both conditions are highlighted in red in the ERP time course plot and delineated with a black line on the topographical map. The time point at which the difference between both conditions is maximal is delineated with a dotted red line in the ERP amplitude time course plot. The electrode at which this difference was obtained is marked with an orange dot on the topographical map.

314 **Cortical responses to rule-based but not feature-based sensory targets are**  
315 **sustained across time in each sensory modality**

316 Previous work has shown that functional differences between cortical responses to  
317 auditory rule-based and feature-based targets are reflected in the extent to which they are  
318 maintained in auditory networks. Cortical activation patterns in response to auditory  
319 rule-based targets are sustained in time, whereas feature-based auditory deviations decay  
320 quickly (King & Dehaene, 2014). Is the temporal evolution of cortical target detection  
321 responses a property common to different sensory domains? We examined whether global  
322 ERP responses are linked to a sustained cortical activation pattern whereas local ERP  
323 responses are supported by short-lived activity regardless of sensory modality. We employed  
324 temporal decoding to characterise neural activation patterns elicited by local and global  
325 ERP responses in different sensory modalities. In short, temporal decoding is a machine  
326 learning approach used to characterise the temporal evolution of cortical activation patterns  
327 linked to sensory events. A classifier trained at a time point  $t$  is not only tested at  $t$  but at  
328 all other remaining time points. This leads to a temporal generalisation matrix of  
329 classification performance scores. The shape of the temporal generalisation matrix offers  
330 insights into the temporal dynamic of cognitive operations and their cortical generators  
331 (Dehaene & King, 2016).

332 We observed that local ERP responses could be decoded along the diagonal in a  
333 mid-range time window for each sensory modality (Figure 3). Across different contrasts, local  
334 ERP responses were found to decay quickly. This finding is mostly consistent with a serial  
335 activation of different cortices dedicated to the sensory modality in which the local ERP  
336 response was applied (King et al., 2014). The visual local ERP response was maintained  
337 briefly between 200-400 ms (mean AUC =  $0.51 \pm 0.03$ , max. AUC = 0.61 at 268 ms training  
338 time and 264 ms testing time, mean cluster  $t = 3.8$ ,  $p < 0.05$ ). In the trimodal study, the  
339 somatosensory local ERP response (mean AUC =  $0.51 \pm 0.02$ , max. AUC = 0.58 at 212 ms

340 training time and 216 ms testing time, mean cluster  $t = 2.96$ ,  $p < 0.05$ ) and the auditory  
341 local ERP response (mean  $AUC = 0.52 \pm 0.03$ , max.  $AUC = 0.67$  at 220 ms training time  
342 and 212 ms testing time, mean cluster  $t = 4.52$ ,  $p < 0.05$ ) were maintained for  $\sim 100$  ms from  
343  $\sim 200$  ms. In the bimodal study, the somatosensory effect was best decoded between 200-300  
344 ms (mean  $AUC = 0.52 \pm 0.03$ , max.  $AUC = 0.63$  at 208 ms training time and 208 ms testing  
345 time, mean cluster  $t = 4.47 \pm 7.53$ ,  $p < 0.05$ ). In this study, temporal decoding revealed a  
346 classification score matrix consistent with two distinct processes underpinning the auditory  
347 local ERP response. From  $\sim 100$  ms, the auditory local ERP response can be decoded along  
348 the diagonal which suggests a serial propagation of cortical activity along the auditory  
349 cortical hierarchy. However, cortical activity is sustained for  $\sim 150$  ms from  $\sim 200$  ms (mean  
350  $AUC = 0.51 \pm 0.04$ , max.  $AUC = 0.71$  at 188 ms training time and 188 ms testing time,  
351 mean cluster  $t = 2.11 \pm 13.15$ ,  $p < 0.05$ ). Although classification scores for the auditory and  
352 somatosensory local ERP response differed from chance across an extended time window,  
353 classifiers performed only slightly better than chance from  $\sim 350$  ms for both effects.

354 We found that classifiers trained to distinguish globally deviant and standard trials  
355 from  $\sim 200$  ms generalised across other time samples in the remaining trial window regardless  
356 of which sensory modality was tested (Figure 3). This decoding procedure led to a  
357 rectangular classification score matrix for each comparison. In line with earlier ERP time  
358 course comparison results (Figure 2), the visual global ERP response manifested relatively  
359 late from  $\sim 400$  ms (mean  $AUC = 0.51 \pm 0.06$ , max.  $AUC = 0.66$  at 516 ms training time  
360 and 520 ms testing time, mean cluster  $t = 3.19$ ,  $p < 0.05$ ). In the trimodal study, the  
361 somatosensory global ERP response appeared from  $\sim 350$  ms ((mean  $AUC = 0.52 \pm 0.05$ ,  
362 max.  $AUC = 0.64$  at 512 ms training time and 508 ms testing time, mean cluster  $t = 5.56$ ,  $p$   
363  $< 0.05$ )) and the auditory global ERP response from  $\sim 200$  ms (mean  $AUC = 0.54 \pm 0.07$ ,  
364 max.  $AUC = 0.69$  at 532 ms training time and 524 ms testing time, mean cluster  $t = 12.5$ ,  $p$   
365  $< 0.05$ ). In the bimodal study, temporal generalisation was found relatively early from  $\sim 150$   
366 ms for both the somatosensory (mean  $AUC = 0.56 \pm 0.06$ , max.  $AUC = 0.7$  at 372 ms

367 training time and 344 ms testing time, mean cluster  $t = 19.32 \pm 19.07$ ,  $p < 0.05$ ) and  
368 auditory global ERP response (mean AUC =  $0.6 \pm 0.05$ , max. AUC = 0.7 at 432 ms  
369 training time and 428 ms testing time, mean cluster  $t = 33.06 \pm 17.56$ ,  $p < 0.05$ ).  
370 Cluster-based permutation tests comparing differences in classification scores between the  
371 local and global ERP response show that the global ERP response generalises in a late time  
372 window whereas the local ERP response does not (Figure 3).

373 Collectively, our results indicate that cortical activation associated with the global  
374 ERP response starts no earlier than  $\sim 150$  ms after onset of the last stimulus in a trial and is  
375 sustained over time until the trial ends. However, we observed some shifts in the onset  
376 latency between different global ERP responses with the visual global ERP response not  
377 appearing before 400 ms. Despite these shifts, this pattern suggests that a single cortical  
378 system is active in that time window (King & Dehaene, 2014). This finding leaves the  
379 question open whether this system is dedicated to a specific sensory modality or shared  
380 between different senses.

### 381 **Supramodal activation is sustained for global but decays for local ERP responses**

382 Here we provide evidence for the hypothesis that cortical hierarchies dedicated to each  
383 sense are organised along a gradient of supramodality. Building up on our finding that global  
384 ERP responses are associated with a sustained late cortical activation pattern, we further  
385 demonstrate that this sustained pattern is shared between different sensory modalities. We  
386 also show that local ERP responses in different sensory modalities rely on few, if any,  
387 common cortical signatures in comparison to global ERP responses.

388 Temporal decoding was employed to examine whether cortical responses share neural  
389 dynamics between sensory modalities. To identify common activity patterns linked to evoked  
390 responses, temporal generalisation analysis can be applied in two ways: Classifiers can be  
391 trained to separate a deviant-standard condition pair in a target sensory modality at a time

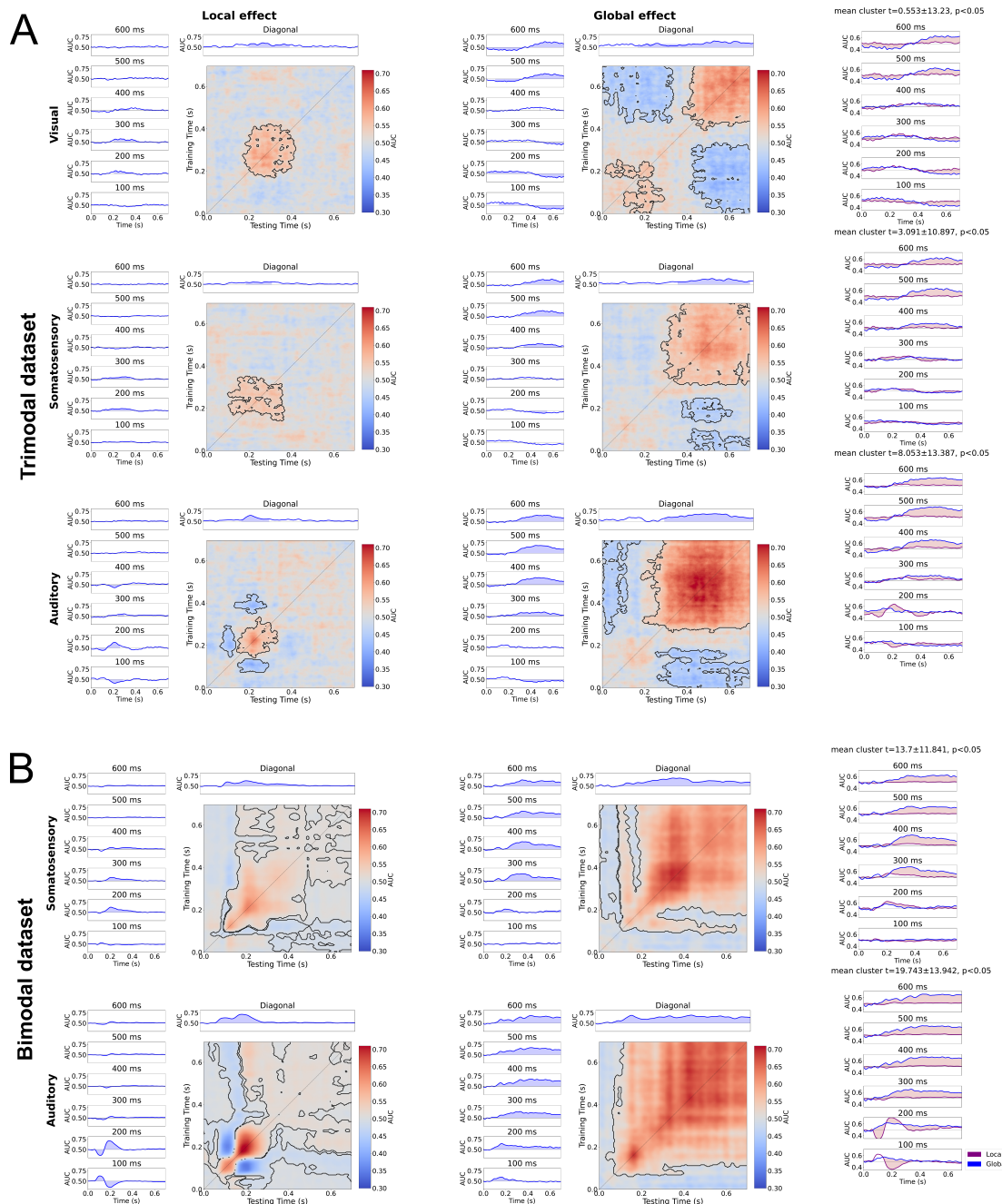


**Figure 3. Temporal generalisation analysis within sensory modalities.** Panels display temporal generalisation results for the local (left) and global ERP response (right) in the trimodal (A) and bimodal dataset (B). Each panel shows results of a temporal generalisation analysis in which a classifier is trained to distinguish deviant and standard trials at each time point and then tested on all remaining time points in a trial. Classification scores are displayed on a red-to-blue gradient. On top of each matrix, adjacent classification scores different from chance (0.5) in a cluster-based permutation test are highlighted with a black line. Next to each matrix, we show a series of time courses of classification scores produced by classifiers trained at the specified time point. On top of each matrix, we plotted the classification score time course for a decoding procedure in which a classifier is trained and tested on deviant-standard pairs at the same time point (corresponding to the matrix diagonal). Classification scores different from chance are highlighted with a blue shade. On the right side, we show results of a cluster-based permutation test contrasting classification score matrices of the corresponding local and global ERP response. Each subplot shows the classification score time courses of a classifier trained to separate global deviant-standard pairs at the specified time point and tested across the remaining time window, and its local counterpart. Time periods in which local and global ERP response classification time courses differ are highlighted in red shade.

392 point t and tested on deviant-standard condition pairs in a different sensory modality across  
393 all time points in a trial. Alternatively, a classifier can be trained to separate  
394 deviant-standard condition pairs when they are pooled across all sensory modalities  
395 separately for global and local ERP responses. We used a 5-fold stratified cross-validation  
396 approach in which classifiers were trained on 4/5 of the data and tested on the remaining 1/5  
397 for both analyses (see Methods for details).

398 We initially trained a classifier to separate globally deviant from standard trials when  
399 trials for each condition pair are pooled across sensory modalities. This procedure revealed  
400 temporal generalisation in a late time window across different global ERP responses in both  
401 datasets (Figure 4). We provide evidence for shared activity supporting the auditory and  
402 visual global ERP response from ~400 ms regardless of whether classifiers were trained on the  
403 visual and tested on the auditory contrast (mean AUC =  $0.52 \pm 0.07$ , max. AUC = 0.66 at  
404 452 ms training time and 572 ms testing time, mean cluster t = 4.62,  $p < 0.05$ ) or vice versa  
405 (mean AUC =  $0.51 \pm 0.06$ , max. AUC = 0.65 at 676 ms training time and 496 ms testing  
406 time, mean cluster t = 3.37,  $p < 0.05$ ). A similar pattern was found for somatosensory and  
407 visual effects when classifiers were trained on visual and tested on somatosensory  
408 deviant-standard pairs (mean AUC =  $0.51 \pm 0.05$ , max. AUC = 0.64 at 540 ms training time  
409 and 464 ms testing time, mean cluster t = 3.2,  $p < 0.05$ ) or vice versa (mean AUC =  $0.51 \pm$   
410 0.07, max. AUC = 0.68 at 580 ms training time and 540 ms testing time, mean cluster t =  
411 2.94,  $p < 0.05$ ). Shared activity between the auditory and somatosensory global ERP  
412 response was found from ~350 ms when classifiers were trained on the auditory and tested on  
413 the somatosensory contrast (mean AUC =  $0.53 \pm 0.05$ , max. AUC = 0.64 at 424 ms training  
414 time and 580 ms testing time, mean cluster t = 10.21,  $p < 0.05$ ) or vice versa (mean AUC =  
415  $0.53 \pm 0.06$ , max. AUC = 0.69 at 576 ms training time and 432 ms testing time, mean  
416 cluster t = 10.26,  $p < 0.05$ ). This finding was replicated in the bimodal dataset in a more  
417 extensive time window from ~150 ms when classifiers were trained on the somatosensory and  
418 tested on the auditory effect (mean AUC =  $0.57 \pm 0.06$ , max. AUC = 0.67 at 188 ms

419 training time and 160 ms testing time, mean cluster  $t = 22.26 \pm 19.85$ ,  $p < 0.05$ ) and vice  
420 versa (mean AUC =  $0.57 \pm 0.05$ , max. AUC = 0.66 at 292 ms training time and 348 ms  
421 testing time, mean cluster  $t = 24.75 \pm 17.7$ ,  $p < 0.05$ ). Taken together, these findings show  
422 that there is shared activation between global ERP responses regardless of which sensory  
423 modality is used for training and testing. The global ERP response consistently manifests in  
424 a rectangular classification score matrix which suggests that common activation is  
425 maintained in cortical networks (with some temporal shifts in onset times).

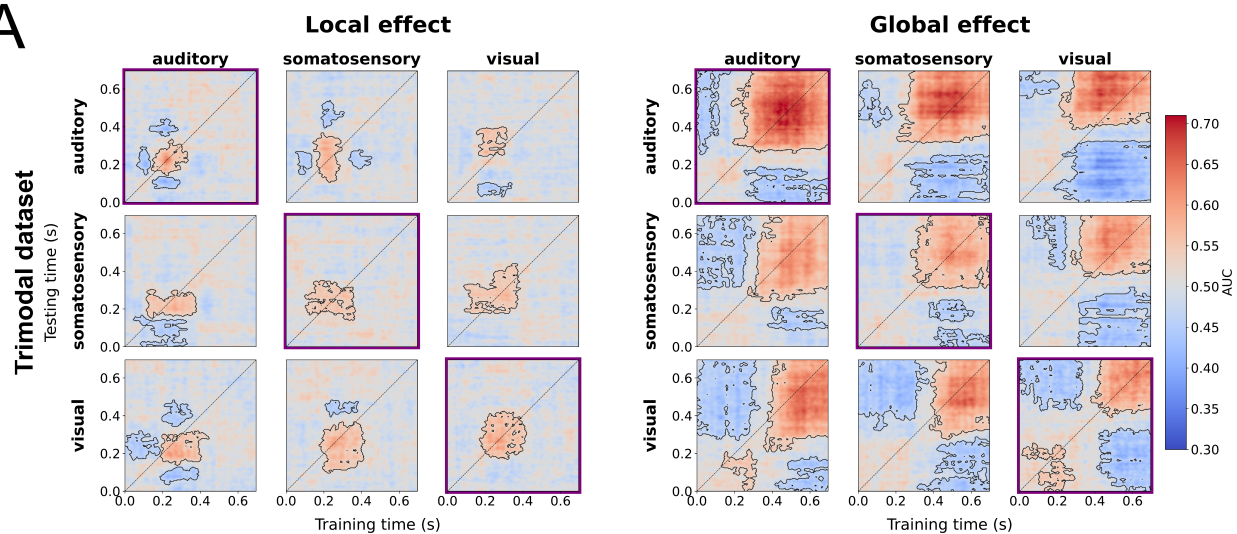
426 Interestingly, temporal decoding of local ERP responses revealed short-lived temporal  
427 generalisation around  $\sim 200$  ms in both datasets. In the trimodal dataset, short-lived shared  
428 representations from  $\sim 200$ -350 ms were found to be associated with local ERP responses  
429 across all comparisons: auditory to somatosensory (mean AUC =  $0.51 \pm 0.03$ , max. AUC =  
430 0.58 at 204 ms training time and 252 ms testing time, mean cluster  $t = 2.04$ ,  $p < 0.05$ ),  
431 somatosensory to auditory (mean AUC =  $0.5 \pm 0.03$ , max. AUC = 0.62 at 216 ms training  
432 time and 200 ms testing time, mean cluster  $t = 1.01$ ,  $p < 0.05$ ), auditory to visual (mean  
433 AUC =  $0.5 \pm 0.03$ , max. AUC = 0.62 at 176 ms training time and 268 ms testing time,  
434 mean cluster  $t = -0.57$ ,  $p < 0.05$ ), visual to auditory (mean AUC =  $0.52 \pm 0.02$ , max. AUC  
435 = 0.59 at 264 ms training time and 192 ms testing time, mean cluster  $t = 4.64$ ,  $p < 0.05$ ),  
436 somatosensory to visual (mean AUC =  $0.5 \pm 0.03$ , max. AUC = 0.6 at 208 ms training time  
437 and 260 ms testing time, mean cluster  $t = 1.34$ ,  $p < 0.05$ ) and visual to somatosensory  
438 (mean AUC =  $0.5 \pm 0.02$ , max. AUC = 0.55 at 260 ms training time and 216 ms testing  
439 time, mean cluster  $t = -0.93$ ,  $p < 0.05$ ). In the bimodal dataset, we found evidence for  
440 shared representations from  $\sim 200$  ms when classifiers were trained on somatosensory and  
441 tested on auditory deviant-standard pairs (mean AUC =  $0.52 \pm 0.03$ , max. AUC = 0.68 at  
442 208 ms training time and 176 ms testing time, mean cluster  $t = 4.9 \pm 9.02$ ,  $p < 0.05$ ) and  
443 vice versa (mean AUC =  $0.51 \pm 0.02$ , max. AUC = 0.64 at 172 ms training time and 208 ms  
444 testing time, mean cluster  $t = 2.99 \pm 8.74$ ,  $p < 0.05$ ).

445 Our result demonstrates that local ERP responses are supported by supramodal

446 transient activation patterns starting from ~200 ms. Although our finding is compatible with  
447 the idea that local ERP responses are processed in cortical hierarchies dedicated to the  
448 sensory modality in which the stimulation is applied, we provide evidence for some overlap in  
449 higher-order or associative regions between these hierarchies. In sum, these results support  
450 the hypothesis that global ERP responses share sustained neural activation patterns between  
451 the senses while local ERP responses share fewer, if any, activity (Figure 4).

452 To corroborate these findings, we use temporal decoding to examine the temporal  
453 evolution of cortical activity when global deviant-standard pairs and local deviant-standard  
454 pairs are each pooled across sensory modalities. Our results show that the local ERP  
455 response is associated with some temporal generalisation from ~180-250 ms in both the  
456 bimodal (mean AUC =  $0.51 \pm 0.02$ , max. AUC = 0.65 at 204 ms training time and 204 ms  
457 testing time, mean cluster  $t = 2.75 \pm 8.43$ ,  $p < 0.05$ ) and the trimodal dataset (mean AUC =  
458  $0.51 \pm 0.03$ , max. AUC = 0.57 at 220 ms training time and 220 ms testing time, mean  
459 cluster  $t = 3.87$ ,  $p < 0.05$ ). For local ERP responses, our result is consistent with the  
460 involvement of a series of modality-specific neural generators in early levels of the cortical  
461 hierarchy and a contribution of supramodal regions in later stages. Again, temporal  
462 decoding revealed sustained shared activation starting from ~150 ms until trial end for the  
463 global ERP response in the bimodal dataset (mean AUC =  $0.579 \pm 0.057$ , max. AUC =  
464 0.667 at 340 ms training time and 336 ms testing time). In the trimodal dataset, shared  
465 activation between global ERP responses extended across the complete time window. We  
466 found evidence for sustained activity from ~350 until trial end. Our results also reveal a  
467 rectangular classification score cluster which differs slightly but significantly from chance  
468 from the onset of the last stimulus in a trial to ~250 ms (mean AUC =  $0.52 \pm 0.06$ , max.  
469 AUC = 0.66 at 520 ms training time and 544 ms testing time, mean cluster  $t = 7.35$ ,  $p <$   
470 0.05). Based on work by King et al. (King & Dehaene, 2014), these temporal generalisation  
471 results suggest that there is a common generator for global ERP responses in different  
472 sensory modalities. In contrast, multiple neural generators support the local ERP response.

**A**



**B**

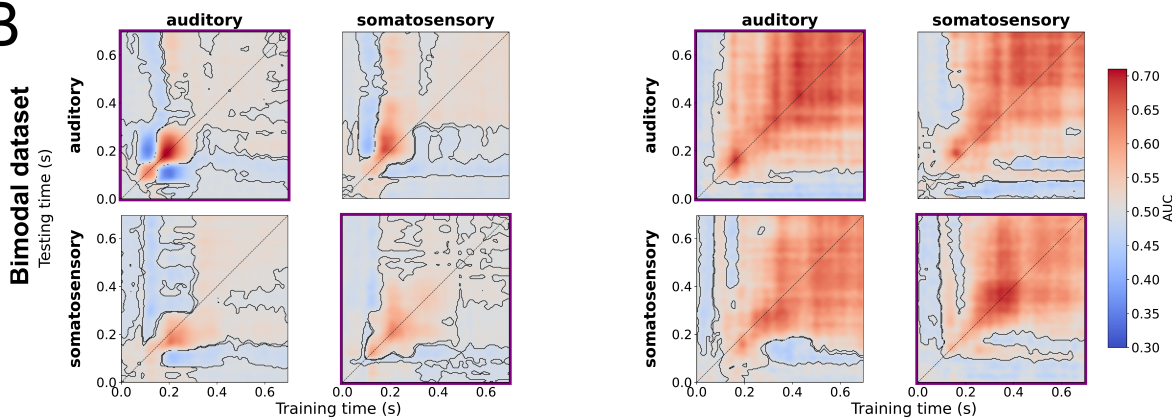


**Figure 4. Temporal generalisation analysis within and between sensory modalities.** Each panel shows results from a series of temporal generalisation analyses decoding the local ERP response (left) and the global ERP response (right) in the trimodal dataset (A) and bimodal dataset (B). Each matrix shows results of a temporal generalisation analysis in which a classifier is trained to distinguish deviant and standard trials at each time point in the training modality and then tested on all remaining time points in a trial in the testing modality. For each experiment, this leads to an  $n$ -by- $n$  matrix with  $n$  being the number of sensory modalities tested in a study (3 for the trimodal and 2 for the bimodal study). Temporal generalisation matrices placed along the diagonal of a panel show results from a decoding analysis performed within a sensory modality and are highlighted with a purple frame. The remaining temporal generalisation matrices show results from a decoding procedure in which a classifier is trained to distinguish deviant and standard trials corresponding to the sensory modality indicated next to each row and tested on the sensory modality corresponding to the column label. AUC-ROC classification scores are shown on a red-to-blue gradient. Classification score clusters which were found to be different from chance in a cluster-based permutation test are delineated with a black line. 0 ms describes the onset of the last stimulus in a trial.

473 For the local ERP response, our evidence shows that these generators are modality-specific  
474 in early stages and supramodal in later stages of cortical processing

475 Finally, we examined differences in decoding strength and cluster size between the local  
476 and global ERP response. For that, we compared maximum classification scores as well as  
477 the number of AUC scores with decoding performance above chance in clusters identified by  
478 the cluster-based permutation test of decoding performance scores drawn from all 14  
479 temporal decoding analyses using Mann-Whitney U tests. Cluster size was enhanced for the  
480 global ERP response relative to the local ERP response ( $U = 2$ ,  $p < 0.001$ ), which suggests  
481 that activation in supramodal networks supporting the global ERP response is sustained in  
482 time, whereas supramodal signatures of the local ERP response decay quickly (Figure 5).  
483 Peak decoding performance was also found to be larger for the global than the local ERP  
484 response ( $U = 36$ ,  $p = 0.001$ ), indicating that decoding results for supramodal activation  
485 linked to the global ERP response are relatively more informative.

486 **Discussion**

487 **Hierarchically nested sensory targets elicit local and global ERP responses  
488 across sensory modalities**

489 A long-standing debate in neuroscience revolves around which sensory and perceptual  
490 processes are supramodal or modality-specific (Cao, Summerfield, Park, Giordano, & Kayser,  
491 2019; Driver & Noesselt, 2008; Faivre, Filevich, Solovey, Kühn, & Blanke, 2018; Walz et al.,  
492 2013). Inspired by the notion that perceptual systems in the cortex are hierarchically  
493 organised on a simple-to-complex axis (Dürschmid et al., 2016; Kiebel et al., 2008; Murray,  
494 2004; Rao & Ballard, 1999), we investigated whether cortical responses to sensory targets  
495 implemented in successive levels of the cortical hierarchy are ordered along a gradient of  
496 supramodality. Across a series of two local-global experiments combining evidence from the  
497 somatosensory, visual and auditory modality, we first established that selective hierarchically

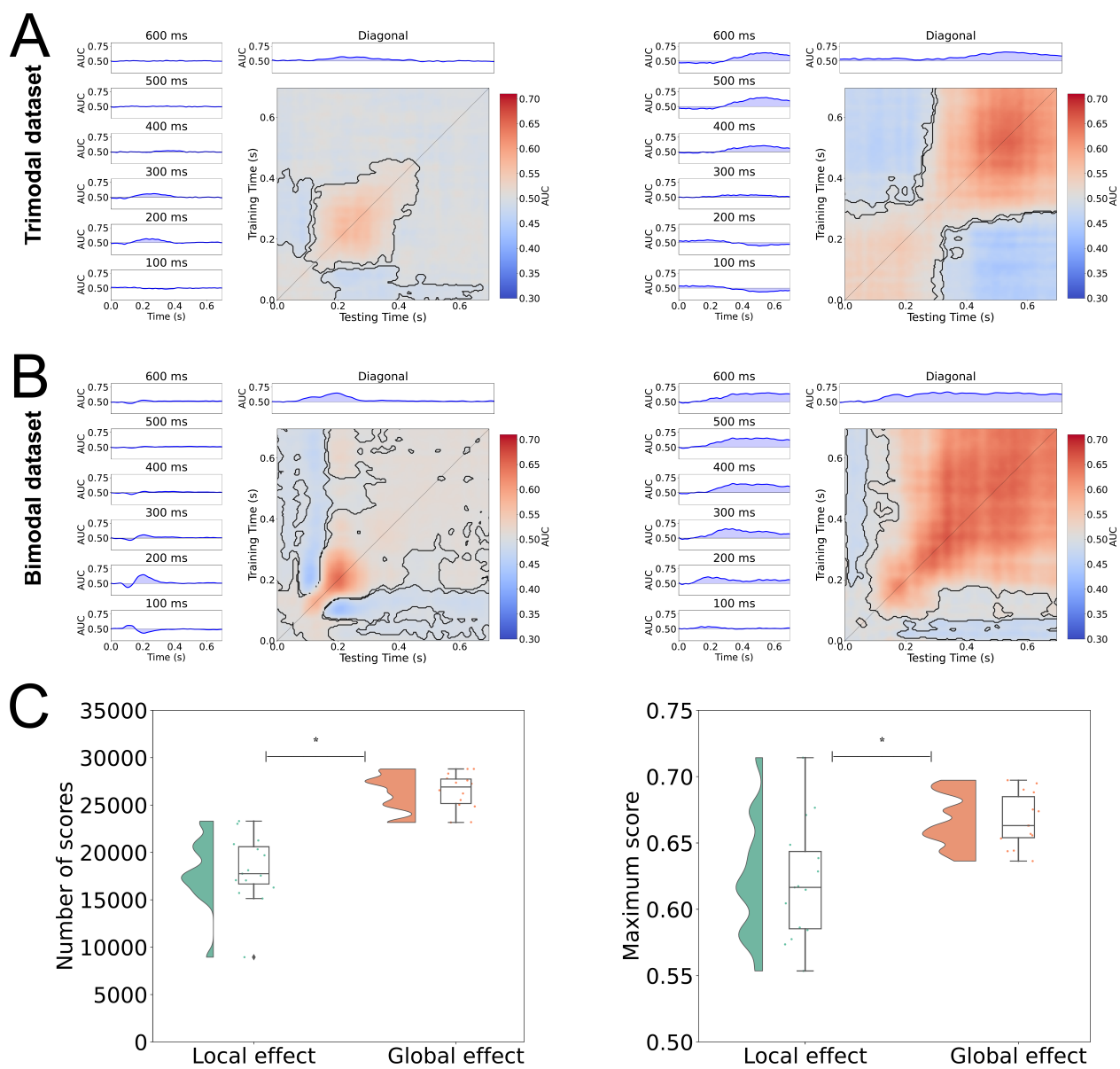
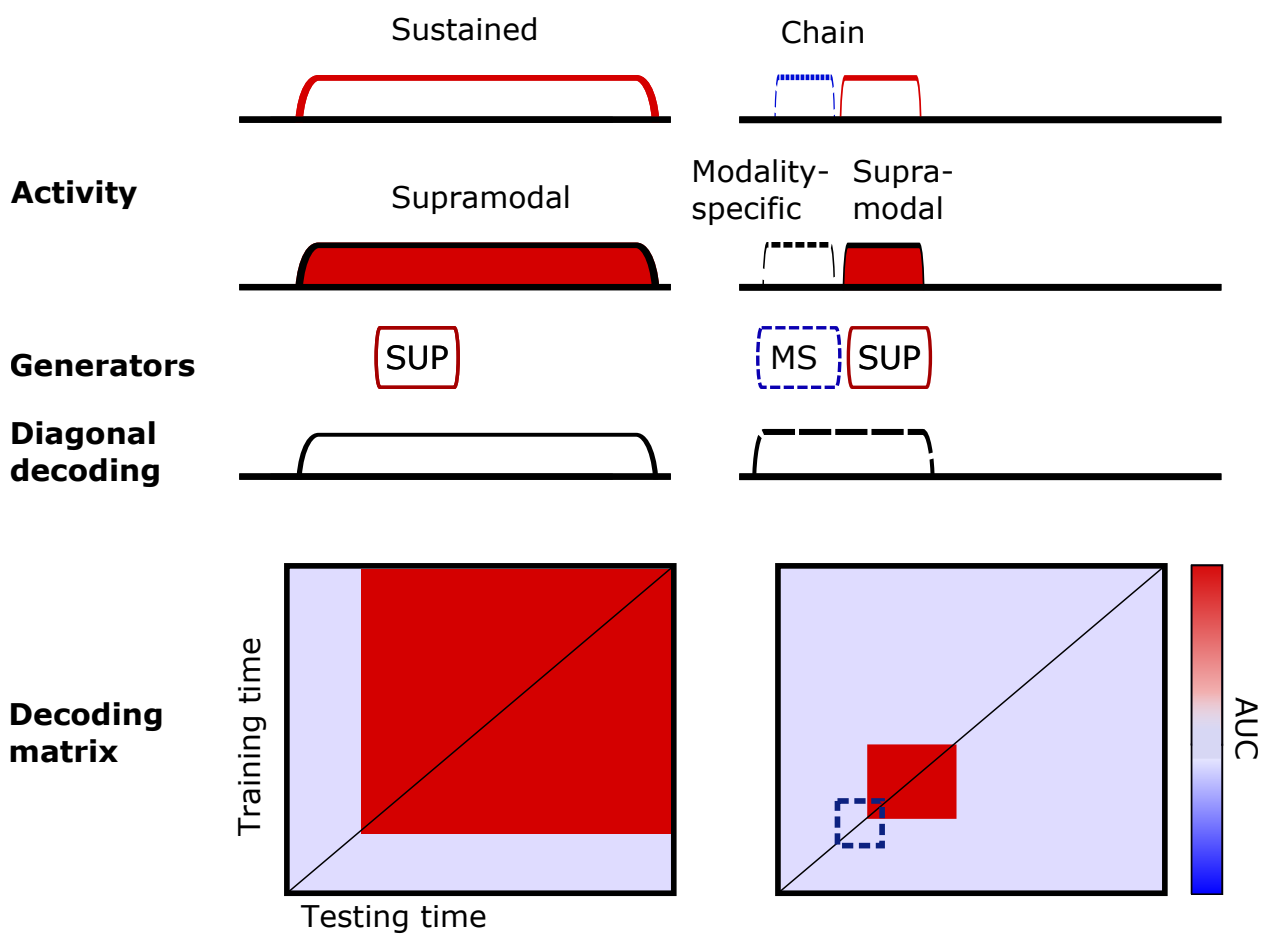


**Figure 5. Temporal decoding of combined sensory modalities.** In a temporal decoding analysis, we pooled deviant trials and standard trials regardless of sensory modality and tested whether a classifier trained to discriminate deviant and standard trials at a specific time point might generalise to the remaining time points. Each panel shows the resulting matrix of AUC-ROC classification scores for the global (A) and local ERP response (B). In each panel, results for the global ERP response are shown on the right and results for the local ERP response are displayed on the left. In conditions in which cluster-based permutation was performed, clusters which differ from chance are highlighted with a purple horizontal line for classification performance in intervals of 100 ms and green for diagonal classification performance. 0 ms marks the onset of the last stimulus in a trial. Clusters of AUC-ROC scores which differed from chance were delineated with a dotted line. Rain cloud plots supplemented with box-and-whisker plots show the distribution of maximum classification scores (right) and number of classification scores above chance in each cluster (left) drawn from clusters across all 14 temporal decoding analyses for the local and global ERP response. Significant differences between the local and global ERP response were assessed with a Mann-Whitney U Test and highlighted with an asterisk (C).



SUP = supramodal

MS = modality-specific

**Figure 6. Summary.** Supramodal and modality-specific aspects of the local and global ERP response. A temporal decoding analysis within sensory modality shows that the global ERP response is supported by one sustained process whereas the local ERP response likely relies on a chain of processes. Follow-up temporal decoding analyses from one modality to the other, and combining all sensory modalities, revealed that the global ERP response activates a single supramodal network across time whereas the local effect is propagated along the cortical hierarchy in a series of short-lived modality-specific and supramodal processes. We infer that a single supramodal generator contributes to the global ERP response whereas the local effect is likely supported by a chain of modality-specific and supramodal generators. Cortical activity indexing the global ERP response leads to an extended rectangular classification score matrix and some classification score clusters ordered along the diagonal. Supramodal processes found in temporal cross-decoding between sensory modalities are highlighted in red and modality-specific processes are shown in blue. We also show a list of supramodal and modality-specific properties of the local and global ERP response (King & Dehaene, 2014).

498 nested divergences of sensory inputs can trigger an MMN-like local ERP response and a  
499 P3b-like global ERP response in different sensory modalities. Most research on the MMN  
500 and P3b concentrates on the auditory domain, and comparably less is known about the  
501 visual or somatosensory P3b or MMN and their temporal dynamics (Linden et al., 1999;  
502 Ostwald et al., 2012). As has been shown for the auditory modality (King et al., 2014), the  
503 global ERP response is maintained in higher-order cortical networks while the local ERP  
504 response is serially propagated along cortical areas which locates both signals at successive  
505 stages in the cortical hierarchy. We show that cortical responses to sensory targets rely on  
506 activation patterns which are sustained in higher-order cortices across time only when  
507 sensory targets are complex and require the attentional tracking of the target for different  
508 sensory modalities. Conversely, the detection of targets which deviate from a short preceding  
509 stimulus stream and require only short-term memory produce a cortical signal which is  
510 propagated along cortical regions in a mid-latency time window regardless of sensory  
511 modality. Converging results from different temporal decoding analyses, we conclude that  
512 the prolonged maintenance of cortical activation elicited by the global ERP response and the  
513 serial propagation of the local ERP response are principles of cortical function found across  
514 sensory modalities. This demonstrates that cortical hierarchies implement target detection  
515 processes which track sensory irregularities in hierarchically nested different timescales at  
516 successive cortical processing stages for each sense.

517 **517 Rule-based sensory targets elicit supramodal and sustained responses in the  
518 cortex**

519 Our finding that the sustained common supramodal activation patterns support the  
520 P3-like global ERP response contributes evidence to a controversy around its putative  
521 supramodal underpinnings. Some studies investigating cortical activation linked to the  
522 auditory and visual P3 suggest a common network including the insula and frontoparietal  
523 areas between these senses (Linden et al., 1999; Walz et al., 2013). However, other studies

524 highlight a contribution of modality-specific higher-order regions to the P300 (Bledowski et  
525 al., 2004), leaving the question open whether and which sensory modalities share cortical  
526 networks to support P3-like global cortical signals. Our results support the notion that a  
527 supramodal (auditory, visual, somatosensory) network underpins the P3-like global ERP  
528 response while at the same time not ruling out contributions of modality-specific processes.

529 Complementing evidence that intrinsic neural timescales are linked to conscious  
530 information processing (Zilio et al., 2021), the global ERP response has also been proposed  
531 to be a cortical signal reflecting the conscious processing of incoming sensory stimulation  
532 (Bekinschtein et al., 2009). By this view, the global ERP response reflects recurrent  
533 information flow in a global neuronal workspace which maintains cortical signatures to  
534 become consciously accessible (Dehaene & Changeux, 2011). Sensory inputs from  
535 modality-specific cortices are fed forward to the global neuronal workspace which broadcasts  
536 integrated multisensory information from the top down to the levels below (Mashour,  
537 Roelfsema, Changeux, & Dehaene, 2020). Our observation that cortical signatures  
538 supporting the global ERP response are supramodal aligns with the theory that the global  
539 ERP response marks a supramodal top-down-driven process in which sensory information is  
540 amplified for conscious access via allocated attention (Chennu et al., 2013).

541 **541 Local ERP responses to sensory targets are linked to short-lived  
542 modality-specific activation**

543 A classic view of MMN-like local ERP responses states that they rely on  
544 modality-specific cortical networks involving primary and secondary sensory regions (Nyman  
545 et al., 1990; Pazo-Alvarez et al., 2003). In our study, temporal cross-decoding analyses  
546 uncovered short-lived supramodal signatures for the local ERP response starting from ~200  
547 ms after onset of the last stimulus in a trial. Interestingly, previous studies demonstrate that  
548 local ERP responses are supported by a network involving modality-specific and frontal  
549 regions in which neuronal messages are propagated forward to the inferior frontal gyrus after

550 initial processing in primary sensory areas, raising the possibility that frontal contributions  
551 to the MMN might host supramodal signatures. Indeed, both the visual and auditory MMN  
552 were found to consist of an earlier component in modality-specific early sensory cortices  
553 followed by an attention-modulated late frontal component from ~200 ms after oddball onset  
554 (Deouell, 2007; Hedge et al., 2015). Similarly, studies of effective connectivity underpinning  
555 the MMN show that the potential is likely supported by a network spanning primary and  
556 secondary sensory cortices as well as frontal regions in different sensory modalities  
557 (Auksztulewicz & Friston, 2015; Chennu et al., 2016; Fardo et al., 2017; Garrido, Kilner,  
558 Kiebel, & Friston, 2009; Ostwald et al., 2012). Finally, the temporal characteristics of  
559 supramodal signatures supporting the local ERP response are congruent with a contribution  
560 of frontal areas linked to attention and target detection (Garrido et al., 2009a). Combined  
561 with earlier results, our results suggest that the MMN-like local ERP response might consist  
562 of short-lived modality-specific and supramodal components. In sum, this finding provides  
563 evidence for the idea that successive layers in the cortical hierarchy might support  
564 increasingly supramodal processes.

565 **A gradient of supramodality as a principle of cortical organisation**

566 The canonical view of cortical function states that cortical hierarchies implement a  
567 strict unimodal-to-supramodal gradient. According to this view, supramodal processing is  
568 deferred to associative and frontal cortices (Felleman & Van Essen, 1991). Mounting  
569 evidence demonstrates that multisensory processes are ubiquitous in the cortical hierarchy  
570 and occur at all processing stages which refutes the idea that early cortices are strictly  
571 unimodal (Driver & Noesselt, 2008; Ghazanfar & Schroeder, 2006). Integrating both views,  
572 our findings support the view that the cortex is hierarchically organised along a gradient of  
573 supramodality. Earlier studies employed the local-global paradigm to demonstrate that the  
574 MMN-like local ERP response is generated in the primary auditory cortex whereas the  
575 global ERP response relies on activity in frontoparietal regions (Bekinschtein et al., 2009;

576 Chao et al., 2018; Chennu et al., 2013; El Karoui et al., 2015; Uhrig, Dehaene, & Jarraya,  
577 2014; Wacongne et al., 2011). In our study, feature-based sensory irregularities triggering  
578 quickly decaying and early modality-specific processes were supplemented by a supramodal  
579 contribution (Figure 6). Finally, a sustained late response to rule-based sensory irregularities  
580 shared between sensory modalities might reflect a recurrent supramodal process in  
581 higher-order cortical areas. However, our finding that local responses evolve into short-lived  
582 supramodal activation patterns provide evidence for the notion that early cortical function is  
583 not strictly specific to a sensory modality. Crucially, our finding that the P3b-like global  
584 ERP response relies on sustained supramodal cortical signatures while the local ERP  
585 response elicits early responses with short-lived commonalities between the senses supports  
586 the notion of a gradient of supramodality underpinning cortical hierarchies but also refutes  
587 the idea that early cortical target detection processes are strictly modality-specific.

588 Finally, our results can be interpreted as evidence for a predictive coding view of  
589 cortical function. Predictive coding states that cortical responses to irregular sensory  
590 information reflect a prediction error resulting from a reconciliation of actual sensory inputs  
591 and their predictions (Clark, 2013; Friston, 2005; Hohwy, 2012; Rao & Ballard, 1999). From  
592 this perspective, local and global ERP responses can be seen as manifestations of prediction  
593 errors located at temporally dissociable successive levels of a dedicated cortical hierarchy for  
594 each sense (Wacongne et al., 2011). A central idea in predictive coding is that higher-order  
595 levels of the cortical hierarchy converge information from different senses forwarded from the  
596 levels below to generate predictions about the sensory environment (Clark, 2013; de Lange et  
597 al., 2018; Friston, 2005; Hohwy, 2012). This aligns with our result that higher-order cortical  
598 responses share supramodal signatures between the senses while lower-order responses largely  
599 rely on modality-specific activation patterns. Extending these earlier findings, we deliver an  
600 integrative framework for cortical responses to sensory targets tracking different time-scales  
601 at successive levels of the cortical hierarchy across different sensory modalities.

602

### Code accessibility

603

Code can be accessed here:

604

<https://github.com/marianiedernhuber/Sustained-supramodal-signatures-target-detection>

605

## References

606 Akatsuka, K., Wasaka, T., Nakata, H., Kida, T., & Kakigi, R. (2007). The effect of stimulus  
607 probability on the somatosensory mismatch field. *Experimental Brain Research*, 181(4),  
608 607–614. <https://doi.org/10.1007/s00221-007-0958-4>

609 Allen, M., Fardo, F., Dietz, M. J., Hillebrandt, H., Friston, K. J., Rees, G., & Roepstorff, A.  
610 (2016). Anterior insula coordinates hierarchical processing of tactile mismatch responses.  
611 *NeuroImage*, 127, 34–43. <https://doi.org/10.1016/j.neuroimage.2015.11.030>

612 Auksztulewicz, R., & Friston, K. (2015). Attentional Enhancement of Auditory Mismatch  
613 Responses: A DCM/MEG Study. *Cerebral Cortex*, bhu323.  
614 <https://doi.org/10.1093/cercor/bhu323>

615 Bekinschtein, T. A., Dehaene, S., Rohaut, B., Tadel, F., Cohen, L., & Naccache, L. (2009).  
616 Neural signature of the conscious processing of auditory regularities. *Proceedings of the  
617 National Academy of Sciences*, 106(5), 1672–1677.  
618 <https://doi.org/10.1073/pnas.0809667106>

619 Bledowski, C., Prvulovic, D., Hoechstetter, K., Scherg, M., Wibral, M., Goebel, R., &  
620 Linden, D. E. J. (2004). Localizing P300 Generators in Visual Target and Distractor  
621 Processing: A Combined Event-Related Potential and Functional Magnetic Resonance  
622 Imaging Study. *Journal of Neuroscience*, 24(42), 9353–9360.  
623 <https://doi.org/10.1523/JNEUROSCI.1897-04.2004>

624 Cao, Y., Summerfield, C., Park, H., Giordano, B. L., & Kayser, C. (2019). Causal Inference  
625 in the Multisensory Brain. *Neuron*, 102(5), 1076–1087.e8.  
626 <https://doi.org/10.1016/j.neuron.2019.03.043>

627 Çatal, Y., Gomez-Pilar, J., & Northoff, G. (2022). Intrinsic Dynamics and Topography of  
628 Sensory Input Systems. *Cerebral Cortex*, bhab504.  
629 <https://doi.org/10.1093/cercor/bhab504>

630 Chang, A. Y.-C., Seth, A. K., & Roseboom, W. (2017). Neurophysiological signatures of  
631 duration and rhythm prediction across sensory modalities. *bioRxiv*, 183954.

632 Chao, Z. C., Takaura, K., Wang, L., Fujii, N., & Dehaene, S. (2018). Large-Scale Cortical  
633 Networks for Hierarchical Prediction and Prediction Error in the Primate Brain. *Neuron*,  
634 100(5), 1252–1266.e3. <https://doi.org/10.1016/j.neuron.2018.10.004>

635 Chennu, S., Noreika, V., Gueorguiev, D., Blenkmann, A., Kochen, S., Ibanez, A., ...  
636 Bekinschtein, T. A. (2013). Expectation and Attention in Hierarchical Auditory  
637 Prediction. *Journal of Neuroscience*, 33(27), 11194–11205.  
638 <https://doi.org/10.1523/JNEUROSCI.0114-13.2013>

639 Chennu, S., Noreika, Gueorguiev, Shtyrov, Bekinschtein, & Henson, R. (2016). Silent  
640 Expectations: Dynamic Causal Modeling of Cortical Prediction and Attention to Sounds  
641 That Weren't. *Journal of Neuroscience*, 36(32), 8305–8316.  
642 <https://doi.org/10.1523/JNEUROSCI.1125-16.2016>

643 Clark, A. (2013). Whatever next? Predictive brains, situated agents, and the future of  
644 cognitive science. *Behavioral and Brain Sciences*, 36(03), 181–204.

645 Cornella, M., Leung, S., Grimm, S., & Escera, C. (2012). Detection of simple and pattern  
646 regularity violations occurs at different levels of the auditory hierarchy. *PLoS One*, 7(8),  
647 e43604. <https://doi.org/10.1371/journal.pone.0043604>

648 Czigler, I., Winkler, I., Pató, L., Várnagy, A., Weisz, J., & Balázs, L. (2006). Visual  
649 temporal window of integration as revealed by the visual mismatch negativity  
650 event-related potential to stimulus omissions. *Brain Research*, 1104(1), 129–140.  
651 <https://doi.org/10.1016/j.brainres.2006.05.034>

652 de Lange, F. P., Heilbron, M., & Kok, P. (2018). How Do Expectations Shape Perception?  
653 *Trends in Cognitive Sciences*, 22(9), 764–779. <https://doi.org/10.1016/j.tics.2018.06.002>

654 Dehaene, S., & Changeux, J.-P. (2011). Experimental and Theoretical Approaches to  
655 Conscious Processing. *Neuron*, 70(2), 200–227.  
656 <https://doi.org/10.1016/j.neuron.2011.03.018>

657 Dehaene, S., & King, J.-R. (2016). Decoding the Dynamics of Conscious Perception: The  
658 Temporal Generalization Method. In *Micro-, Meso-and Macro-Dynamics of the Brain*

659 (pp. 85–97). Springer.

660 Deouell, L. Y. (2007). The Frontal Generator of the Mismatch Negativity Revisited. *Journal*  
661 *of Psychophysiology*, 21(3-4), 188–203. <https://doi.org/10.1027/0269-8803.21.34.188>

662 Donner, T., Kettermann, A., Diesch, E., Ostendorf, F., Villringer, A., & Brandt, S. A.  
663 (2000). Involvement of the human frontal eye field and multiple parietal areas in covert  
664 visual selection during conjunction search. *European Journal of Neuroscience*, 12(9),  
665 3407–3414. <https://doi.org/10.1046/j.1460-9568.2000.00223.x>

666 Dreо, J., Attia, D., Pirtošek, Z., & Repovš, G. (2017). The P3 cognitive ERP has at least  
667 some sensory modality-specific generators: Evidence from high-resolution EEG.  
668 *Psychophysiology*, 54(3), 416–428. <https://doi.org/10.1111/psyp.12800>

669 Driver, J., & Noesselt, T. (2008). Multisensory Interplay Reveals Crossmodal Influences on  
670 “Sensory-Specific” Brain Regions, Neural Responses, and Judgments. *Neuron*, 57(1),  
671 11–23. <https://doi.org/10.1016/j.neuron.2007.12.013>

672 Dürschmid, S., Edwards, E., Reichert, C., Dewar, C., Hinrichs, H., Heinze, H.-J., … Knight,  
673 R. T. (2016). Hierarchy of prediction errors for auditory events in human temporal and  
674 frontal cortex. *Proceedings of the National Academy of Sciences*, 113(24), 6755–6760.  
675 <https://doi.org/10.1073/pnas.1525030113>

676 El Karoui, I., King, J.-R., Sitt, J., Meyniel, F., Van Gaal, S., Hasboun, D., … Naccache, L.  
677 (2015). Event-Related Potential, Time-frequency, and Functional Connectivity Facets of  
678 Local and Global Auditory Novelty Processing: An Intracranial Study in Humans.  
679 *Cerebral Cortex*, 25(11), 4203–4212. <https://doi.org/10.1093/cercor/bhu143>

680 Ester, E. F., Serences, J. T., & Awh, E. (2009). Spatially Global Representations in Human  
681 Primary Visual Cortex during Working Memory Maintenance. *Journal of Neuroscience*,  
682 29(48), 15258–15265. <https://doi.org/10.1523/JNEUROSCI.4388-09.2009>

683 Faivre, N., Filevich, E., Solovey, G., Kühn, S., & Blanke, O. (2018). Behavioral, Modeling,  
684 and Electrophysiological Evidence for Supramodality in Human Metacognition. *Journal*  
685 *of Neuroscience*, 38(2), 263–277. <https://doi.org/10.1523/JNEUROSCI.0322-17.2017>

686 Fardo, F., Auksztulewicz, R., Allen, M., Dietz, M. J., Roepstorff, A., & Friston, K. J. (2017).  
687 Expectation violation and attention to pain jointly modulate neural gain in  
688 somatosensory cortex. *Neuroimage*, 153.

689 Felleman, D. J., & Van Essen, D. (1991). Distributed hierarchical processing in the primate  
690 cerebral cortex. *Cerebral Cortex (New York, N.Y. : 1991)*, 1(1), 1–47.  
691 <https://doi.org/10.1093/cercor/1.1.1>

692 Friston, K. (2005). A theory of cortical responses. *Philosophical Transactions of the Royal  
693 Society B: Biological Sciences*, 360(1456), 815–836.  
694 <https://doi.org/10.1098/rstb.2005.1622>

695 Garrido, M. I., Kilner, J. M., Kiebel, S. J., & Friston, K. J. (2009). Dynamic Causal  
696 Modeling of the Response to Frequency Deviants. *Journal of Neurophysiology*, 101(5),  
697 2620–2631. <https://doi.org/10.1152/jn.90291.2008>

698 Garrido, M. I., Kilner, J. M., Stephan, K. E., & Friston, K. J. (2009a). The mismatch  
699 negativity: A review of underlying mechanisms. *Clinical Neurophysiology*, 120(3),  
700 453–463.

701 Garrido, M. I., Kilner, J. M., Stephan, K. E., & Friston, K. J. (2009b). The mismatch  
702 negativity: A review of underlying mechanisms. *Clinical Neurophysiology*, 120(3),  
703 453–463. <https://doi.org/10.1016/j.clinph.2008.11.029>

704 Ghazanfar, A., & Schroeder, C. (2006). Is neocortex essentially multisensory? *Trends in  
705 Cognitive Sciences*, 10(6), 278–285. <https://doi.org/10.1016/j.tics.2006.04.008>

706 Golesorkhi, M., Gomez-Pilar, J., Tumati, S., Fraser, M., & Northoff, G. (2021). Temporal  
707 hierarchy of intrinsic neural timescales converges with spatial core-periphery organization.  
708 *Communications Biology*, 4(1), 1–14. <https://doi.org/10.1038/s42003-021-01785-z>

709 Golesorkhi, M., Gomez-Pilar, J., Zilio, F., Berberian, N., Wolff, A., Yagoub, M. C. E., &  
710 Northoff, G. (2021). The brain and its time: Intrinsic neural timescales are key for input  
711 processing. *Communications Biology*, 4(1), 1–16.  
712 <https://doi.org/10.1038/s42003-021-02483-6>

713 Halgren, E., Baudena, P., Clarke, J. M., Heit, G., Liégeois, C., Chauvel, P., & Musolino, A.  
714 (1995). Intracerebral potentials to rare target and distractor auditory and visual stimuli.  
715 I. Superior temporal plane and parietal lobe. *Electroencephalography and Clinical*  
716 *Neurophysiology*, 94(3), 191–220.

717 Halgren, E., Marinkovic, K., & Chauvel, P. (1998). Generators of the late cognitive  
718 potentials in auditory and visual oddball tasks. *Electroencephalography and Clinical*  
719 *Neurophysiology*, 106(2), 156–164. [https://doi.org/10.1016/S0013-4694\(97\)00119-3](https://doi.org/10.1016/S0013-4694(97)00119-3)

720 Hedge, C., Stothart, G., Todd Jones, J., Rojas Frías, P., Magee, K. L., & Brooks, J. C. W.  
721 (2015). A frontal attention mechanism in the visual mismatch negativity. *Behavioural*  
722 *Brain Research*, 293, 173–181. <https://doi.org/10.1016/j.bbr.2015.07.022>

723 Hohwy, J. (2012). Attention and conscious perception in the hypothesis testing brain.  
724 *Attention and Consciousness in Different Senses*, 74.

725 Ito, T., Hearne, L. J., & Cole, M. W. (2020). A cortical hierarchy of localized and distributed  
726 processes revealed via dissociation of task activations, connectivity changes, and intrinsic  
727 timescales. *NeuroImage*, 221, 117141. <https://doi.org/10.1016/j.neuroimage.2020.117141>

728 Katayama, J., & Polich, J. (1998). Stimulus context determines P3a and P3b.  
729 *Psychophysiology*, 35(1), 23–33.

730 Kiebel, S. J., Daunizeau, J., & Friston, K. J. (2008). A Hierarchy of Time-Scales and the  
731 Brain. *PLOS Computational Biology*, 4(11), e1000209.  
732 <https://doi.org/10.1371/journal.pcbi.1000209>

733 King, J.-R., & Dehaene, S. (2014). Characterizing the dynamics of mental representations:  
734 The temporal generalization method. *Trends in Cognitive Sciences*, 18(4), 203–210.  
735 <https://doi.org/10.1016/j.tics.2014.01.002>

736 King, J.-R., Gramfort, A., Schuriger, A., Naccache, L., & Dehaene, S. (2014). Two Distinct  
737 Dynamic Modes Subtend the Detection of Unexpected Sounds. *PLOS ONE*, 9(1),  
738 e85791. <https://doi.org/10.1371/journal.pone.0085791>

739 Linden, D. E. J., Prvulovic, D., Formisano, E., Völlinger, M., Zanella, F. E., Goebel, R., &

740 Dierks, T. (1999). The Functional Neuroanatomy of Target Detection: An fMRI Study of  
741 Visual and Auditory Oddball Tasks. *Cerebral Cortex*, 9(8), 815–823.  
742 <https://doi.org/10.1093/cercor/9.8.815>

743 Maekawa, T., Goto, Y., Kinukawa, N., Taniwaki, T., Kanba, S., & Tobimatsu, S. (2005).  
744 Functional characterization of mismatch negativity to a visual stimulus. *Clinical*  
745 *Neurophysiology*, 116(10), 2392–2402. <https://doi.org/10.1016/j.clinph.2005.07.006>

746 Mäntysalo, S., & Näätänen, R. (1987). The duration of a neuronal trace of an auditory  
747 stimulus as indicated by event-related potentials. *Biological Psychology*, 24(3), 183–195.

748 Mariola, A., Baykova, R., Chang, A. Y. C., Seth, A. K., & Roseboom, W. (2019). Clear  
749 Evidence for Electrophysiological Signatures of Duration and Rhythm Prediction, but not  
750 across Sensory Modalities. *2019 Conference on Cognitive Computational Neuroscience*.  
751 Berlin, Germany: Cognitive Computational Neuroscience.  
752 <https://doi.org/10.32470/CCN.2019.1389-0>

753 Maris, E., & Oostenveld, R. (2007). Nonparametric statistical testing of EEG- and  
754 MEG-data. *Journal of Neuroscience Methods*, 164(1), 177–190.  
755 <https://doi.org/10.1016/j.jneumeth.2007.03.024>

756 Mashour, G. A., Roelfsema, P., Changeux, J.-P., & Dehaene, S. (2020). Conscious  
757 Processing and the Global Neuronal Workspace Hypothesis. *Neuron*, 105(5), 776–798.  
758 <https://doi.org/10.1016/j.neuron.2020.01.026>

759 Miller, E. K. (2009). Executive Function and Higher-Order Cognition: Definition and Neural  
760 Substrates. *Encyclopedia of Neuroscience*, 4, 7.

761 Murray, C. (2004). An interpretative phenomenological analysis of the embodiment of  
762 artificial limbs. *Disability and Rehabilitation*, 26(16), 963–973.

763 Näätänen, R., Simpson, M., & Loveless, N. E. (1982). Stimulus deviance and evoked  
764 potentials. *Biological Psychology*, 14(1), 53–98.  
765 [https://doi.org/10.1016/0301-0511\(82\)90017-5](https://doi.org/10.1016/0301-0511(82)90017-5)

766 Northoff, G., Wainio-Theberge, S., & Evers, K. (2020). Is temporo-spatial dynamics the

767 “common currency” of brain and mind? In Quest of “Spatiotemporal Neuroscience.”

768 *Physics of Life Reviews*, 33, 34–54. <https://doi.org/10.1016/j.plrev.2019.05.002>

769 Nyman, G., Alho, K., Laurinen, P., Paavilainen, P., Radil, T., Reinikainen, K., ...

770 Nääätänen, R. (1990). Mismatch negativity (MMN) for sequences of auditory and visual  
771 stimuli: Evidence for a mechanism specific to the auditory modality.

772 *Electroencephalography and Clinical Neurophysiology/Evoked Potentials Section*, 77(6),

773 436–444. [https://doi.org/10.1016/0168-5597\(90\)90004-W](https://doi.org/10.1016/0168-5597(90)90004-W)

774 Oostenveld, R., Fries, P., Maris, E., & Schoffelen, J.-M. (2011). FieldTrip: Open Source  
775 Software for Advanced Analysis of MEG, EEG, and Invasive Electrophysiological Data  
776 [Research Article]. <https://www.hindawi.com/journals/cin/2011/156869/>.  
777 <https://doi.org/10.1155/2011/156869>

778 Ostwald, D., Spitzer, B., Guggenmos, M., Schmidt, T. T., Kiebel, S. J., & Blankenburg, F.  
779 (2012). Evidence for neural encoding of Bayesian surprise in human somatosensation.  
780 *NeuroImage*, 62(1), 177–188.

781 Pazo-Alvarez, P., Cadaveira, F., & Amenedo, E. (2003). MMN in the visual modality: A  
782 review. *Biological Psychology*, 63(3), 199–236.  
783 [https://doi.org/10.1016/S0301-0511\(03\)00049-8](https://doi.org/10.1016/S0301-0511(03)00049-8)

784 Pegado, F., Bekinschtein, T., Chausson, N., Dehaene, S., Cohen, L., & Naccache, L. (2010).  
785 Probing the lifetimes of auditory novelty detection processes. *Neuropsychologia*, 48(10),  
786 3145–3154. <https://doi.org/10.1016/j.neuropsychologia.2010.06.030>

787 Phillips, H. N., Blenkmann, A., Hughes, L. E., Kochen, S., Bekinschtein, T. A., Rowe, J.  
788 B.others. (2016). Convergent evidence for hierarchical prediction networks from human  
789 electrocorticography and magnetoencephalography. *Cortex*, 82, 192–205.

790 Polich, J. (2007). Updating P300: An integrative theory of P3a and P3b. *Clinical  
791 Neurophysiology*, 118(10), 2128–2148. <https://doi.org/10.1016/j.clinph.2007.04.019>

792 Rao, R. P., & Ballard, D. H. (1999). Predictive coding in the visual cortex: A functional  
793 interpretation of some extra-classical receptive-field effects. *Nature Neuroscience*, 2(1),

794 79–87.

795 Raut, R. V., Snyder, A. Z., & Raichle, M. E. (2020). Hierarchical dynamics as a macroscopic  
796 organizing principle of the human brain. *Proceedings of the National Academy of  
797 Sciences*, 117(34), 20890–20897.

798 Shen, G., Smyk, N. J., Meltzoff, A. N., & Marshall, P. J. (2018). Using somatosensory  
799 mismatch responses as a window into somatotopic processing of tactile stimulation.  
800 *Psychophysiology*, 55(5), e13030. <https://doi.org/10.1111/psyp.13030>

801 Shirazibeheshti, A., Cooke, J., Chennu, S., Adapa, R., Menon, D. K., Hojjatoleslami, S. A.,  
802 ... Bowman, H. (2018). Placing meta-stable states of consciousness within the predictive  
803 coding hierarchy: The deceleration of the accelerated prediction error. *Consciousness  
804 and Cognition*, 63, 123–142. <https://doi.org/10.1016/j.concog.2018.06.010>

805 Sitt, J. D., King, J.-R., El Karoui, I., Rohaut, B., Faugeras, F., Gramfort, A., ... Naccache,  
806 L. (2014). Large scale screening of neural signatures of consciousness in patients in a  
807 vegetative or minimally conscious state. *Brain*, 137(8), 2258–2270.  
808 <https://doi.org/10.1093/brain/awu141>

809 Squires, K., Petuchowski, S., Wickens, C., & Donchin, E. (1977). The effects of stimulus  
810 sequence on event related potentials: A comparison of visual and auditory sequences.  
811 *Perception & Psychophysics*, 22(1), 31–40. <https://doi.org/10.3758/BF03206077>

812 Taylor, P., Hobbs, J. N., Burroni, J., & Siegelmann, H. T. (2015). The global landscape of  
813 cognition: Hierarchical aggregation as an organizational principle of human cortical  
814 networks and functions. *Scientific Reports*, 5(1), 18112.  
815 <https://doi.org/10.1038/srep18112>

816 Tiitinen, H., May, P., Reinikainen, K., & Näätänen, R. (1994). Attentive novelty detection in  
817 humans is governed by pre-attentive sensory memory. *Nature*, 372(6501), 90.

818 Uhrig, L., Dehaene, S., & Jarraya, B. (2014). A Hierarchy of Responses to Auditory  
819 Regularities in the Macaque Brain. *Journal of Neuroscience*, 34(4), 1127–1132.  
820 <https://doi.org/10.1523/JNEUROSCI.3165-13.2014>

821 Wacongne, C., Labyt, E., van Wassenhove, V., Bekinschtein, T., Naccache, L., & Dehaene, S.  
822 (2011). Evidence for a hierarchy of predictions and prediction errors in human cortex.  
823 *Proceedings of the National Academy of Sciences*, 108(51), 20754–20759.  
824 <https://doi.org/10.1073/pnas.1117807108>

825 Walz, J. M., Goldman, R. I., Carapezza, M., Muraskin, J., Brown, T. R., & Sajda, P. (2013).  
826 Simultaneous EEG-fMRI Reveals Temporal Evolution of Coupling between Supramodal  
827 Cortical Attention Networks and the Brainstem. *Journal of Neuroscience*, 33(49),  
828 19212–19222. <https://doi.org/10.1523/JNEUROSCI.2649-13.2013>

829 Wengler, K., Goldberg, A. T., Chahine, G., & Horga, G. (2020). Distinct hierarchical  
830 alterations of intrinsic neural timescales account for different manifestations of psychosis.  
831 *eLife*, 9, e56151. <https://doi.org/10.7554/eLife.56151>

832 Wolff, A., Berberian, N., Golesorkhi, M., Gomez-Pilar, J., Zilio, F., & Northoff, G. (2022).  
833 Intrinsic neural timescales: Temporal integration and segregation. *Trends in Cognitive  
834 Sciences*, 26(2), 159–173. <https://doi.org/10.1016/j.tics.2021.11.007>

835 Yamaguchi, S., & Knight, R. T. (1991a). Anterior and posterior association cortex  
836 contributions to the somatosensory P300. *Journal of Neuroscience*, 11(7), 2039–2054.

837 Yamaguchi, S., & Knight, R. T. (1991b). P300 generation by novel somatosensory stimuli.  
838 *Electroencephalography and Clinical Neurophysiology*, 78(1), 50–55.

839 Zilio, F., Gomez-Pilar, J., Cao, S., Zhang, J., Zang, D., Qi, Z., ... Northoff, G. (2021). Are  
840 intrinsic neural timescales related to sensory processing? Evidence from abnormal  
841 behavioral states. *NeuroImage*, 226, 117579.  
842 <https://doi.org/10.1016/j.neuroimage.2020.117579>